FEATURE EXTRACTION OF BATHYMETRIC LIDAR WAVEFORMS

Wei-Tsun LIN[a] and Peter Tian-Yuan SHIH[b]

[a]PhD Student, Department of Civil Engineering, National Chiao Tung University, Taiwan.
Tel: + 886-3-5712121#54991; Fax: +886-3-5716257; E-mail: bowlikuan@gmail.com
[b]Professor, Department of Civil Engineering, National Chiao Tung University, Taiwan.
Tel: + 886-3-5712121#54940; Fax: +886-3-5716257; E-mail: tyshih@mail.nctu.edu.tw

KEY WORDS: Function Fitting, Filtering, Empirical Mode Decomposition

Abstract: Bathymetric Lidarprovidesa practical tool for surveying shallow water zone and the area characterized with navigation threats.The backscatter intensity of laser pulses starting from the emission,and then traveling through air and water, to finally reflected from the bottom,is detectedand recorded. This forms waveform.From the timestamps of feature points in the waveform, the corresponding position and depth can be derived. In thisstudy, the waveforms collected from a Dongsha atoll mission with AHAB Hawkeye II systemare investigated. This system has four receiving channels including two greens, one infra-red and one Raman. Waveforms of different depth, ranging from less than 1m to 40m, are selected for the study.Ensemble Empirical mode decomposition (EEMD) method is used to reduce the noises in the waveform. Weibull distribution is used for fitting the filtered waveform for extracting features.The depths are then derived from the time interval between surface and bottom feature points.The resultis compared with the depth derived from the AHAB Coastal Survey Studio (CSS) software.The moment of laser beam reached water surface could be detected from all these four channels. It is found that there is a time offset among them. This may be caused by the different settings of the detection devices between different channels, such as the length of the signal transmission cable. These offsets certainly should be calibrated in a lab environment.

1. INTRODUCTION

Bathymetric Lidar, also called Airborne LidarBathymetry (ALB), can measure the water depthby using green channel laser, which iscapableof penetrating water effectively.Some ALB systems use multi-channel devices, which record the green, infra-red and Raman channel, can provide more accurate result and suitable for a variety of surveying conditions.Although green laser pulse can penetrate the water then providebackscatter and bottom information in the corresponding waveform, the surface return is embedded in the volume backscatter and is hard to define accurately.Therefore, the infra-red and Raman are usedfor the determination of water surface.

There are several approaches proposed for the return pulse detection from Lidar waveform (Allouis et al., 2010; Pe'eri and Philpot, 2007). The function fitting methods are often used because the fitted function provides not only timestamp of return pulse but also the featuresof pulse shape. And these features may be used for further applications. In this study, function fitting method is applied to the depth estimation. And the reprocessing procedure is included.

2. EXPERIMENTAL DATA

In this study, waveforms are derived from anAHAB HawkEye II system, which can be operatedfor both topographic and hydrographic surveying. The scanning devices are mounted on the aircraft with 400m flight height, 150 knots speed, andthe resulting point density is 3.5m×3.5m . This system provides the vertical accuracy with 0.25m, and the ability of depth measuring from 0.3m to 3 times of Secchidisk depth. HawkEye II system emits wavelength 1064nm infra-red and 532nm green channels, and receives two green channels, one infra-red channel and one Raman channel. Two green channels are detected by Avalanche Photo Diodes (APDs) and Photo Multiplier Tubes (PMTs), which are used for the shallow channel and deep channel respectively. Moreover, the received green channel signals are applied with the time-varied gain (TVG) to enhance the bottom return signal and compensate the signal attenuation due to the depth. Figure 1 exemplifies the TVG (red line) and the processed green channel waveform (black line).

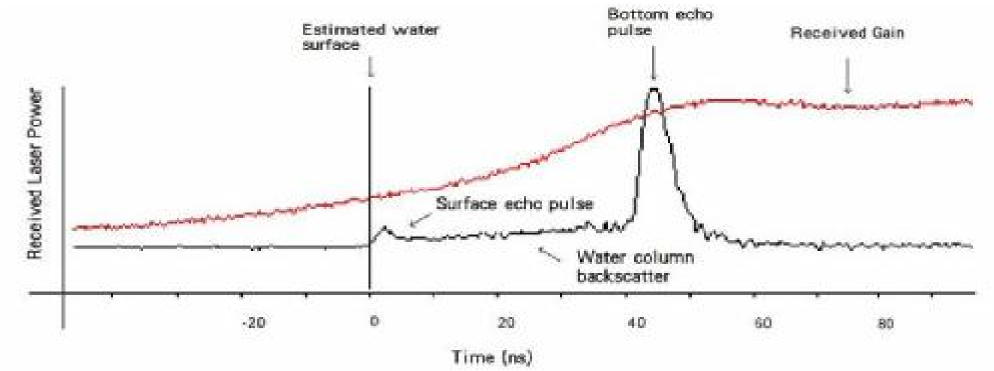

Figure 1:TVG of HawkEye II green channel waveforms (Liu et al., 2010)

The point clouds of 7 areas with different depth are selected. Thedepth of these areas ranges from within 1m to about 40m. And the depths in each area are relatively similar. The information of the total 710 point cloud selected in this study is listed in Table 1.

Table 1: Information of selected point cloud

Area	1	2	3	4	5	6	7
Number of point(pts)	113	123	113	63	95	76	127
Depth from CSS(m)	0.27~ 0.91	1.02~ 2.48	11.17~ 14.34	15.38~ 16.06	18.07~ 19.94	31.22~ 32.29	39.12~ 40.74

3. METHODOLOGY

The computation of water depth from Lidar waveforms requires the detection of timestamps atboth water surface and bottom. The detailed processingscheme is as following.

3.1 Ensemble EMD

Empirical mode decomposition(EMD) method is necessary to deal with data from non-stationary and nonlinear processes (Huang and Shen, 2005).The decomposition is based on the assumption that data consists of different simple intrinsic modes of oscillation. Each intrinsic mode represents simple oscillation, which is represented by an intrinsic mode function (IMF) with the following definition: (1) the number of extrema and the number of zero-crossings must either equal or differ at one; (2) the mean value of the envelope defined by the local maxima and the envelope defined by the local minima is zero in any point.The EMD method includes several repetition of sifting process. And the final outcomes are the IMFs indifferent frequency. The ensemble EMD was proposed by Wu and Huang (2009). It can solve the mode mixing problem that EMD does not work very well (Wu and Huang, 2009).

Figure 2 shows an example of green channel waveform processed withEEMD (Ensemble Empirical Mode Decomposition). The blue lines are the IMFs and the frequency decreased from top to bottom. To reduce the high frequency noise, the waveform is reconstructed from the second to eighth IMFs (red line in Figure 2).

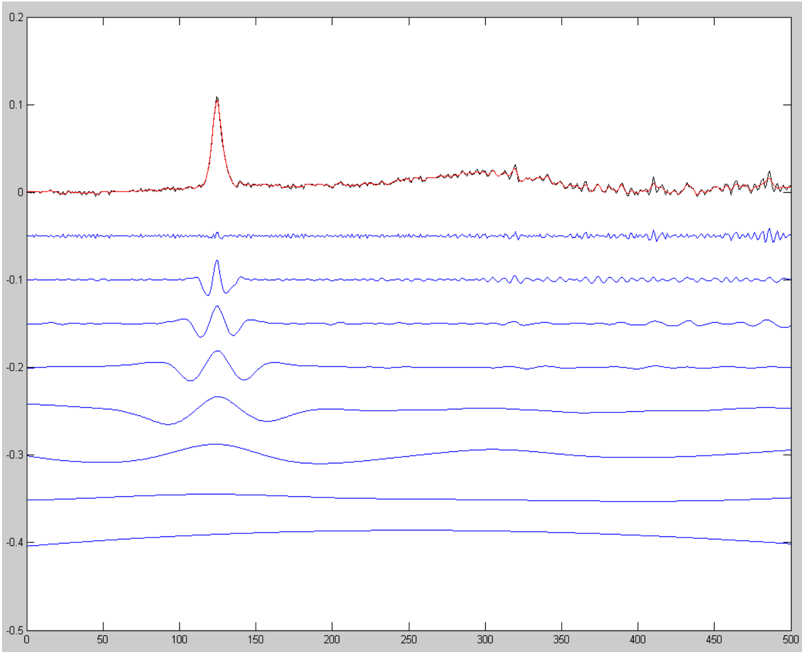

Figure2: Example of IMFs by EEMD

3.2 Depth Estimation

After the filtering procedure with the EEMD method, the timestamps of water surface and the bottom are derived from function fitting. In this study, trust region algorithm was used to fitting the filtered waveforms. This algorithm can provide the initial value of the fitting function and reduce the probability of fitting error.

The HawkEye II system provides 2 green channels, which both can provide bottom timestamp in the depth surveying. Based on the signal to noise ratio (SNR), the one with better signal quality is selected from the two green channels.Moreover, the offset between four channels due to the different setting of detection devices is computed. The depth is computed after the timestamp offsets between channels are corrected.

3.2.1 Peak Detection

Generally, the maximum value of green channel signal value reveals on the bottom return of the waveform (see Figure 1). But some cases are not due to water quality condition. To providegoodinitial value for the fitting function, the position fitted return pulse need to be determined. During the differentiation of signal, the zero crossing between maximum and minimum of differentiated signal is corresponding to the peak position of origin signal (Wong and Antonious, 1994). The differentiation procedure is easily affected by noise, so the filtering processing in advance is need.

3.2.2 Function Fitting

The Weibull distribution function is used in this study. It can be symmetric or asymmetric (Mallet et al., 2009). The formula of Weibull distribution function is listed in (3-1).

$$a \times \frac{k}{\lambda}\left(\frac{x-s}{\lambda}\right)^{k-1} \times \exp\left(-\left(\frac{x-s}{\lambda}\right)^{k}\right) \qquad (3\text{-}1)$$

x: time (nanosecond)
a: amplitude
k: scale parameter
λ: shape parameter

The fitting function provides the position and other information of fitted pulse, while the feature point indicate the pulse return position in the function is need further defined. Several definitions of return pulse position such as 50% rise time, center of gravity, peak, mean and midpoint (Abshire et al., 1994), and the 50% rise time is used in this study.

3.2.3 Signal Offset

To find the offset between channel devices, we tried to detect the surface return pulse from the four channels. And the timestamp differences between channels are estimated by the statistic result. The green channels of Hawk Eye II system are applied with TVG processing, which make the surface return less obvious. In our test, there's 96points that the surface return from green channels both are detected. The statistic results are listed in Table 2. Overall, the surface return from IRchannel is late than the one from green channel about 30ns, and Raman channel is late than the green channel about 40ns (see Figure 3). While the mean of difference between two green channels is about 1.5ns, the difference is ignored. These above result are taken into account for the depth computation.

Table 2: Statistic difference results of surface return between channels

Unit(ns)	IR-Shallow	Raman-Shallow	IR-Deep	Raman-Deep
Mean	29.710	39.359	28.728	37.059
Standard deviation	7.337	14.989	8.348	13.193

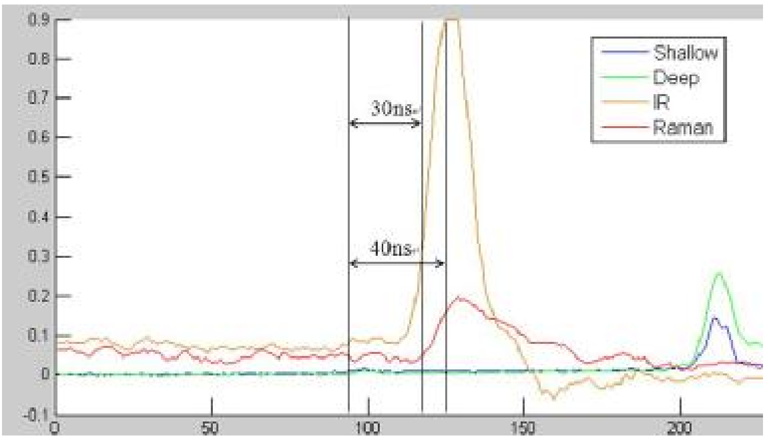

Figure 3: The offset between channels

3.2.4 Depth Computation

HawkEye II system scans with laser beam about 19 degree tilting angle forward. Therefore, the travelling distance in water of laser beam can be calculated by the timestamps of surface and bottom in the waveforms, which is the slant range. The water depth then needs the further correction according to the Snell's law. The depths are derived by the time interval from surface and bottom times the velocity of light in water and divided by 2. And the incident angle for each laser beams are applied to the slant correction. The velocity of light in water is 225400 km/s (Allouis et al., 2010), and the refraction coefficient is 1.341 (Billard et al., 1986).

There are two green channels for the determination of bottom return. SNR of green channels are computed and choose the one with better performance. The SNR and utilizationpercentage of green channels are listed in the Table 3. In our study, the waveform from moderate depth mainly uses the shallow channel, while deep channel is mainly used in deep depth.

Table 3: SNR and utilization of green channel

	1	2	3	4	5	6	7
Mean SNR of shallow channel(dB)	10.89	8.73	9.83	10.65	9.31	6.25	6.94
Mean SNR of deep channel(dB)	8.90	8.97	7.46	7.08	7.23	7.71	7.18
Utilization of shallow channel (%)	66	47	100	100	100	14	16

4. RESULT

Estimated depths are computed with the four channels. The water surface returns are determined by the IR and Raman channel, and the bottom returns are detected by the green channels. The result of our estimation is compared with the depth from CSS software. Table 4 and Table 5 are the depth estimation result with the surface return timestamps from IR and Raman channel, respectively. The mean error is the mean of difference by CSS depth minus estimated depth. In the area 1, mean error and standard deviation are -0.1, 0.54 and 0.81, 0.52 by IR and Raman, respectively. The performance is not well in the area with depth shallower than 1m. The mean error and standard deviation increasesignificantly when the depth larger than 20m (area 6, 7).

Table 4: Depth estimation result in each area (surface channel: IR)

	1	2	3	4	5	6	7
Mean Error (m)	-0.1	0.07	0.03	-0.07	0.97	1.82	3.82
Standard deviation (m)	0.54	0.54	0.89	1.03	1.17	2.10	4.91

Table 5: Depth estimation result in each area (surface channel: Raman)

	1	2	3	4	5	6	7
Mean Error (m)	0.81	0.07	0.09	0.08	1.05	2.12	4.06
Standard deviation (m)	0.52	0.59	0.87	1.00	1.16	2.10	4.92

Figure 4 shows the linear regression of CSS depth and estimated depth. And the dot lines in the figure are the line with slope equal to 1. The slopes of regression line are 0.930 and 0.924. In the area 6 and 7, the underestimation of depth is much significant. The R^2 of linear regression in whole data is 0.989.

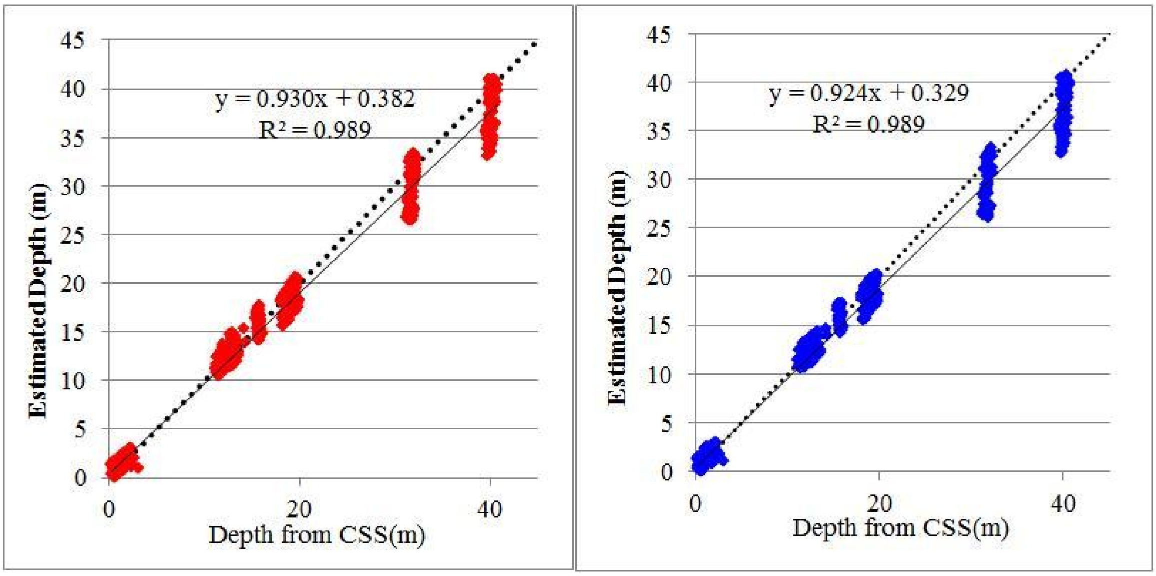

Figure4: Regression of CSS depth and estimated depth using IR (left) and Raman channel

5. CONCLUSION AND DISCUSSION

This research uses the waveforms of HawkEye II bathymetric Lidar to estimate water depth in Dongsha atoll. The mean errorsrelative to CSS computed aregenerally increased with depth. However, the result in area 1 is not consistent with this trend. The estimation of shallow water depth needsto be further investigated.While the characteristics of each channel are quite different, the waveforms of each channel might require different scheme.

REFERENCES:

Abshire, J. M., McGarray,J.F. Pacini,L.K. Blair,J.B. and Elman,C.G., 1994.LaserAltimetry Simulator version 3.0, User's Guide, NASA Technical Memorandum 104588, 66 p.

Allouis, T., Bailly, J-S., Pastol Y. and Le Roux, C., 2010.Comparison of LiDAR Waveform Processing Methods for Very Shallow Water Bathymetry Using Raman, Near-infrared, and Green Signals. Earth Surface Processes and Landforms Vol. 35, No. 6, pp. 640-650.

Billard, B., Abbot, R.H. and Penny, M. F., 1986.Modeling Depth Bias in an Airborne Laser Hydrographic System, Applied Optics, Vol. 25, No. 13, pp.2089-2098.

Huang, N. E., and Shen, S. S. P., 2005.Hilbert-HuangTransform and Its Applications, 311 pp., World Sci., Singapore.

Liu, X., Tulldahl, H. M., and Axelsson, A., 2010. Bathymetry LiDAR Reflectance Processing and Seafloor Classification. Proceeding of European LiDAR Mapping Forum, Netherlands, 30 Nov-1 Dec.

Mallet, C., Lafarge, F., Bretar, F., Roux, M., Soergel, U. and Heipke, C., 2009.A Stochastic Approach for Modeling Airborne LiDAR Waveforms.

Pe'eri, S. and Philpot, W., 2007.Increasing the Existence of Very Shallow-water LiDAR Measurements Using the Red-channel Waveforms. IEEE Transactions on Geoscience and Remote Rensing, Vol. 45, No. 5, pp. 1217-1223.

Wong, H. C. and Antonious, A., 1994.One-dimensional Signal Processing Techniques for Airborne Laser Bathymetry, IEEE Transactions on Geoscience and Remote Sensing, Vol. 32, No. 1, pp. 35-46.

Wu, Z. H and Huang,N. E. 2009. Ensemble Empirical Mode Decomposition : A Noise-Assisted Data Analysis Method , Advances in Adaptive Data Analysis, Vol. 1, No. 1, pp. 1-41.